IOP Publishing Journal of Physics: Condensed Matter

J. Phys.: Condens. Matter **23** (2011) 115302 (7pp) doi:10.1088/0953-8984/23/11/115302

Spin relaxation in semiconductor quantum rings and dots—a comparative study

Elżbieta Zipper[1], Marcin Kurpas[1], Janusz Sadowski[2,3] and Maciej M Maśka[1]

[1] Institute of Physics, University of Silesia ul. Uniwersytecka 4, 40-007 Katowice, Poland
[2] MAX-Lab, Lund University, SE-221 00 Lund, Sweden
[3] Institute of Physics, Polish Academy of Sciences, al. Lotnikow 32/46, 02-668 Warszawa, Poland

E-mail: maciej.maska@us.edu.pl

Received 11 November 2010, in final form 5 February 2011
Published 3 March 2011
Online at stacks.iop.org/JPhysCM/23/115302

Abstract

We calculate spin relaxation times due to spin–orbit-mediated electron–phonon interactions for experimentally accessible semiconductor quantum ring and dot architectures. We elucidate the differences between the two systems due to different confinement. The estimated relaxation times (at $B = 1$ T) are in the range between a few milliseconds to a few seconds. This high stability of spin in a quantum ring allows us to test it as a spin qubit. A brief discussion of quantum state manipulations with such a qubit is presented.

(Some figures in this article are in colour only in the electronic version)

1. Introduction

Small nanostructures are physical systems which allow a controlled study of confined quantum spin dynamics in a solid. In particular, the spin of a single-electron semiconductor quantum dot (QD) placed in a magnetic field $\boldsymbol{B}$ is a natural two-level system suitable for use as a qubit [1, 2]. Strong confinement present in QDs leads to a drastic reduction of spin–phonon coupling mediated by a combination of electron–phonon and spin–orbit interactions (SOI) which results in relaxation times exceeding seconds [3–5].

Quantum confinement properties of QDs can be deeply mutated to crater-like nanostructures (in other words, to ring-shaped QDs) called hereafter quantum rings (QRs) [6–11]. The ability to fill a QR with one or a few electrons offers new possibilities, e.g. to detect the persistent current (PC) carried by single-electron states [10] or the magneto-induced Bohm–Aharonov change of the ground state [8, 9]. It was found [12] that nanorings with $R < 20$ nm can be considered as almost ideal quantum systems and thus can be important in quantum information processing. Recently some proposals on how to build quantum gates on QRs have been given [13, 14]. The orbital states in QRs are strongly quantized and therefore the electron spin states are expected to be very stable due to the substantial suppression of spin-flip mechanisms.

It is just interesting to study how differences in quantum confinement (geometry, electron distribution) for QDs and QRs translate into relaxation times for these structures.

Electron spin decoherence is caused primarily by spin–lattice relaxation via phonon scattering and spin–orbit interaction and by hyperfine interaction (HFI) with nuclear spins [5, 15]. At magnetic fields $B < 0.1$ T the dominant relaxation mechanism is the HFI but for larger fields this mechanism is suppressed by the mismatch between the nuclear and electron Zeeman energies. At $0.5\ \text{T} < B < 10$ T the SOI causes spin relaxation by mixing the spin and orbital states and providing the mechanism for coupling of spins to (mainly) piezoelectric phonons [16, 17]. Throughout this paper we assume $B = 1$ T and discuss spin relaxation induced by the Dresselhaus SO coupling that emerges from the absence of inversion asymmetry of GaAs-type crystals.

The considerations in this paper are general and can be used for rings produced by (i) methods relying on self-assembled growth (SQRS) [8–11] and (ii) methods using nanolithographical procedures and electrostatic potentials (EQRs) [3, 6]. The calculated relaxation times are long enough to treat QRs with one or a few electrons as a spin qubit.

In section 2 we introduce basic characteristics of quantum rings. In section 3 we make estimations of the relaxation and decoherence times, while in section 4 we discuss the formation of spin qubits and provide a brief description of how

to manipulate their states. A general discussion is given in section 5.

2. Quantum confinement of semiconductor quantum rings

We consider a semiconductor QR of radius r_0 and finite thickness containing a single or a few electrons. The ring is placed in a static homogeneous magnetic field parallel ($B_\parallel$) or perpendicular ($B_\perp$) to its plane. The in-plane orientation is favorable as it does not reduce the distance between the orbital levels.

For a 2D ring in a magnetic field $B_\perp$ in the confining potential $V(r)$ and phonon potential $V_{\rm ph}$ we assume the Hamiltonian is in the form

$$H = H_R + \frac{e\hbar}{2m^*}\hat{\boldsymbol{\sigma}}\cdot\boldsymbol{B} + H_{\rm SO} + V_{\rm ph} \tag{1}$$

where

$$H_{\rm SO} = \beta\left(-\hat{\sigma}_x p_x + \hat{\sigma}_y p_y\right) \tag{2}$$

is the Dresselhaus SO interaction due to the bulk inversion asymmetry,

$$H_R = \frac{1}{2m^*}(\mathbf{p} + e\boldsymbol{A})^2 + V(r), \tag{3}$$

describes an electron in the ring, m^* is the effective electron mass and $\boldsymbol{A} = (0, xB_z, 0)$ is the vector potential. The exact form of $V(r)$ will be given later in the text. If the ring is placed in a parallel magnetic field $B_\parallel$ instead of $B_\perp$ then $\boldsymbol{A} = 0$. $H_{\rm SO}$ provides a small admixture of a state with the opposite spin to each orbital state with spin up or down and gives the electron spin the opportunity to relax.

The energy spectrum of H_R consists of a set of discrete levels $E_{\rm nl}$ due to radial motion with radial quantum numbers $n = 0, 1, 2, \ldots$, and rotational motion with angular momentum quantum numbers $l = 0, \pm1, \pm2, \ldots$. The single-particle wavefunction is of the form

$$\Psi_{\rm nl} = R_{\rm nl}(r)\exp(\mathrm{i}l\phi)\,\chi_\sigma, \tag{4}$$

with the radial part $R_{\rm nl}(r)$ and the spin part χ_σ. For finite-width QRs both $E_{\rm nl}$ and $\Psi_{\rm nl}$ have to be calculated numerically [18]. In contrast to QDs, the energy levels numbered by $n > 0$ always lie higher in energy than those with increasing l and they do not enter the following analysis.

The application of a magnetic field $\boldsymbol{B}$ splits the orbital energy levels by

$$\Delta_Z = g_s\mu_B B, \tag{5}$$

where g_s is the electron spin g factor and μ_B is the Bohr magneton. Another important energy gap is the distance from the highest occupied orbital state (l) to the first excited orbital state ($l \pm 1$):

$$\Delta_l = \begin{cases} E_{0,l\pm1} - E_{0,l}, & \text{for } B = B_\parallel, \\ E_{0,l-1} - E_{0,l}, & \text{for } B = B_\perp. \end{cases} \tag{6}$$

If the following relation holds

$$k_B T \ll \Delta_Z \ll \Delta_l, \tag{7}$$

Table 1. Relaxation times calculated for three modeled InGaAs quantum rings corresponding (in alphabetical order) to the experimental rings described in [8–10]. The ring geometry has been reached by the confining potential $V_1(r)$ (equation (8)); $\hbar\omega_0$ is the potential strength. $B_\parallel = 1$ T has been assumed.

Ring	r_0 (nm)	$\hbar\omega_0$ (meV)	T_1^0 (s)	T_1^1 (s)	T_1^2 (s)	T_1^3 (s)
A	20	15	0.015	0.053	0.067	0.071
B	14	12	0.26	0.19	0.14	0.11
C	11.5	25	1.35	1.88	1.66	1.36

the two Zeeman sublevels of the orbital l are well separated from the others and the ring can be well approximated as a two-state system (a qubit). We assume that the 'operating' orbital l is occupied by a single electron only, i.e. for $l = 0$ the number of electrons is $N_e = 1$, for $|l| = 1$, $N_e = 3$, etc.

In our analysis we consider several different quantum rings. The radii and confining potentials of three of them (A, B and C) are chosen to roughly reproduce the energy spectra of the recently grown InGaAs rings described in [8–10], respectively. The confining potential used in all these cases is assumed to be of the following form:

$$V_1(r) = \tfrac{1}{2}m^*\omega_0^2(r - r_0)^2, \tag{8}$$

where the parameters are collected in table 1.

For the remaining rings we have assumed the same radius as for ring B, but the potential takes on different shapes. In order to be able to compare results for QRs and QDs, we parameterize the potential in such a way that it can reproduce both the harmonic potential of a QD as well as a δ-like potential of a quasi-one-dimensional 1D QR. It is given by

$$\begin{aligned} V_2(r) &= \frac{1}{2}m^*\omega_0^2\left[(1-k)r^2 + \frac{k}{1-k}(r - r_0)^2\right] \\ &= \tfrac{1}{2}m^*\omega_{\rm QD}^2 r^2 + \tfrac{1}{2}m^*\omega_{\rm QR}^2(r - r_0)^2. \end{aligned} \tag{9}$$

It is a superposition of QD and QR potentials, where the confinement (a measure of radial localization of the electron wavefunction) is given by $\hbar\omega_{\rm QD}$ and $\hbar\omega_{\rm QR}$, respectively. For $k = 0$ the second term vanishes and the potential describes a harmonic QD. On the other hand, in the $k \to 1$ limit it describes a 1D QR. Therefore, changing k from 0 to 1 one can observe how the properties of a quantum system evolve while moving from a QD to QR. The radius of a QR is defined by r_0 in equation (8), i.e. it is the distance from the center of the ring to the minimum of the confining potential. The definition of the radius of a harmonic QD is not so unambiguous—we use r_0 defined by the shape of the ground state wavefunction $\Psi(r, \phi) \propto \exp(-r/r_0)$. In order to ensure that the size of the system does not depend on k, and therefore that its properties depend only on the shape of the potential, in equation (9) we assume

$$\omega_0 = 2\hbar/m^* r_0^2, \tag{10}$$

which gives the radius of the QD equal to r_0. Figure 1 shows the radial part of the wavefunction for the ground state ($l = 0$) and four lowest excited states ($l = 1, \ldots, 4$) for different values of k: for $k = 0$ we model a QD (figure 1(a)), while for $0 < k < 1$ we get QRs of decreasing thickness (figures 1(b) and (c)), reaching at $k = 0.999$ a quasi-1D ring (figure 1(d)).

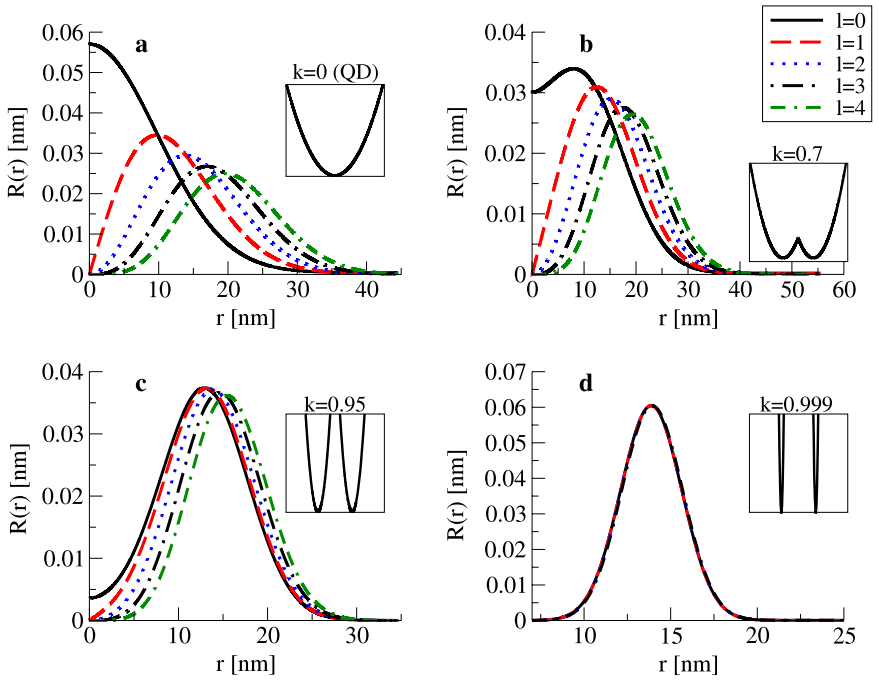

Figure 1. The radial part $R_{0l}(r)$ of the electron wavefunction (4) plotted as a function of radius r for different values of the orbital quantum number l. Panels (a)–(d) include results for different shapes of the confining potential (9) (shown in the inset plots). In all cases $r_0 = 14$ nm, $B_\parallel = 1$ T have been assumed.

We would like to stress that our model calculations are for the circularly symmetric nanostructures, whereas some of the experimentally fabricated rings may have slightly different symmetry and therefore a slightly different energy spectrum. Additionally, we neglect any imperfectnesses that are present in real rings (impurities, variable thickness, etc).

As the experiments were performed mainly at $B \geqslant 1$ T, in the following we fix the magnitude of the magnetic field to $B = 1$ T. We also assume the electron spin g factor $|g_s| = 0.8$ for InGaAs samples [4], which gives the electron spin Zeeman splitting $\Delta_Z = 0.046$ meV.

3. Spin relaxation and decoherence

The comprehensive analysis of relaxation in QDs is given in [16, 17]. It was shown that at $B = 1$ T relaxation is dominated by a single-phonon admixture process governed by H_{SO} (equation (2)) in good agreement with experiments [3–5, 19]. To discuss the relaxation we follow [16] and in particular equation (7) in this paper, which is valid for a set of confining potentials and therefore for different shapes of the sample.

The formula for the relaxation time T_1^l is of the form

$$\frac{1}{T_1^l} = 2C_{\rm ph}(\alpha_{xx}^l)^2(1+\cos^2\vartheta)\Delta_z^5, \tag{11}$$

where $\vartheta = 0$ for $B = B_\perp$, $\vartheta = \pi/2$, $B = B_\parallel$; the exact form of $C_{\rm ph}$ is given in [16]

$$\alpha_{xx}^l = \sum_{l''} 2e^2 \frac{|\langle 0, l''|x|0, l\rangle|^2}{E_{0,l''} - E_{0,l}} = \frac{4\pi^2 e^2}{\Delta_l}\Xi_l^2, \tag{12}$$

where 0 stands for the quantum number n, l is the orbital number of the highest occupied state and

$$\Xi_l = \int_0^\infty R_{0l}^* R_{0l'} r^2\,{\rm d}r, \tag{13}$$

is the 'overlap factor', where R_{0l} is the radial part of the electron wavefunction (4) and $l' = l - 1$ if the field is perpendicular to the ring or $l' = l \pm 1$ for a parallel field.

Applying a little algebra one obtains the relaxation time for a spin in the highest occupied state l:

$$T_1^l = \frac{\eta}{\Delta_z^5}\frac{\Delta_l^2}{\Xi_l^4}, \tag{14}$$

where

$$\eta = \frac{\hbar^5}{\Lambda_{\rm p}(2\pi)^4(m^*)^2(1+\cos^2\vartheta)}, \tag{15}$$

$\Lambda_{\rm p}$ is a dimensionless constant depending on the strength of the effective spin-piezoelectric phonon coupling and the magnitude of SOI, $\Lambda_{\rm p} = 0.007$ for GaAs-type systems [4, 16].

In contrast to QDs, where $\Delta_l = \hbar\omega_0$, for QRs Δ_l increases with increasing l (faster for a thinner ring), tending to

$$\Delta_l^{\rm 1D} = \frac{\hbar^2}{2m^* r_0^2}(2l+1), \tag{16}$$

for a quasi-1D ring (see figure 2(a)).

It is interesting to compare the relaxation times for QRs and QDs (solid black lines in figures 2(a)–(c)). For a single electron ($l = 0$) we get for a QD

$$T_1^{0,\rm dot} = \Lambda_{\rm p}^{-1}\frac{\hbar\,(\hbar\omega_0)^4}{(\Delta_Z)^5\,(1+\cos^2\vartheta)}, \tag{17}$$

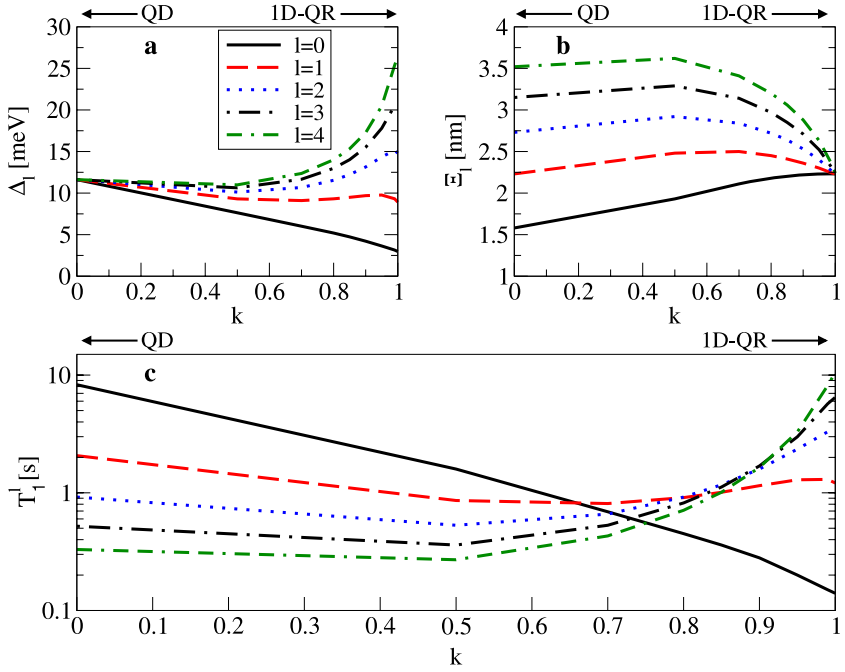

Figure 2. (a) The orbital energy gap Δ_l as a function of the potential parameter k, for different values of l (corresponding to different occupation N_e). For $k = 0$ the potential (equation (9)) models QD and Δ_l is l-independent. Increasing k we reach (for $k \to 1$) the 1D QR limit with Δ_l defined by equation (16); (b) the overlap factor Ξ_l and (c) the relaxation time T_1 plotted as a function of k for different orbital states l. $r_0 = 14$ nm has been assumed.

i.e. the relaxation time for QDs obtained in [16], whereas for QR

$$T_1^0 = T_1^{0,\mathrm{dot}} \left(\frac{\Delta_0}{\hbar\omega_0}\right)^2 \left(\frac{\Xi_0^{\mathrm{dot}}}{\Xi_0}\right)^4, \qquad \left(\Xi_0^{\mathrm{dot}}\right)^2 = \frac{\hbar^2}{4\pi^2 m^* \hbar\omega_0}. \tag{18}$$

We find out that

$$\left.\begin{array}{l}\hbar\omega_0 > \Delta_0,\\ \Xi_0^{\mathrm{dot}} < \Xi_0\end{array}\right\} \Rightarrow T_1^0 < T_1^{0,\mathrm{dot}}, \tag{19}$$

i.e. $T_1^{0,\mathrm{dot}}$ is a higher limit of T_1^0 for arbitrary ring thickness.

To understand the first of the inequalities we compare the formulae for Δ_0 for QD (equation (10)) and 1D QR (equation (16)). We see that $\hbar\omega_0 = 4\Delta_0^{1\mathrm{D}}$. For rings of finite thickness Δ_0 changes smoothly between these two values.

The inequality between the overlap factors Ξ_0 and Ξ_0^{dot} follows from the difference in shape and distribution of the radial parts R_{0l} (figures 1(a)–(d)). For QD the radial functions are concentrated closer to $r = 0$ than for QRs where they stay mostly at larger r. Additionally, for QD the difference between the $R_{00}(r)$ and $R_{01}(r)$ is much more significant than for QR. Both these properties result in a smaller value of Ξ_0 for a QD than for a QR, leading to the relations (19).

Notice that the relation (19) is a consequence of the assumed parabolic shape of the potential confining both the QDs and QRs. For a rectangular potential, for example, the charge distribution of the electrons would be different, leading to the decrease of the difference between T_1^0 and $T_1^{0,\mathrm{dot}}$.

The situation, however, changes if the number of electrons is larger than one. It was shown [5, 6] that for such cases the electron–electron interaction is well approximated by the constant interaction model—it shifts the single-electron spectra by a multiple of the charging energy, $(N_e - 1)E_C$. Assuming this, the spectra in figures 2 and 3 correspond to the energies after the charging energy has been subtracted.

One can see from figure 1(a) that for QDs with $l > 0$ the maxima of the wavefunctions move to larger r leading to an increase of Ξ_l^{dot} (figure 2(b)) and a subsequent decrease of T_1^{dot} (figure 2(c)). For QRs of large thickness ($0 < k < 0.8$) the situation is similar as for QDs, but for thinner rings with $k > 0.8$ both the decrease of Ξ_l (figure 2(b)) and the simultaneous increase of Δ_l (figure 2(a)) lead to a substantial increase of T_1^l (see figure 2(c) and table 2). In table 1 we also presented the relaxation times for the rings A–C. We see that they increase considerably with decreasing radius of the rings, reaching a value of $T_1^0 = 1.35$ s already for a singly occupied ring C. However, because rings A–C are relatively thick we do not get the essential increase of T_1^l for $l > 0$. It follows from our calculations that rings with $r_0 \leqslant 10$ nm have relaxation times strongly exceeding 1 s.

The results presented in figure 2 and table 2 have been obtained for the magnetic field parallel to the ring. In such a case the movement of electrons is not affected by the field, which results in a twofold degeneracy of orbital states $E_{0,l} = E_{0,-l}$. This degeneracy is removed when there is a non-zero component of the magnetic field perpendicular to the ring. Then, $E_{0,-|l|} < E_{0,|l|}$ and the distance to the first excited state has to be calculated according to the lower line in equation (6). It leads to smaller values of Δ_l than for the field parallel to the QR. Since the overlap factor Ξ_l is very weakly modified by the perpendicular field (figure 3(b)), the relaxation time given by equation (14) is reduced but still $T_1 \geqslant 1$s for $l > 0$ is accessible

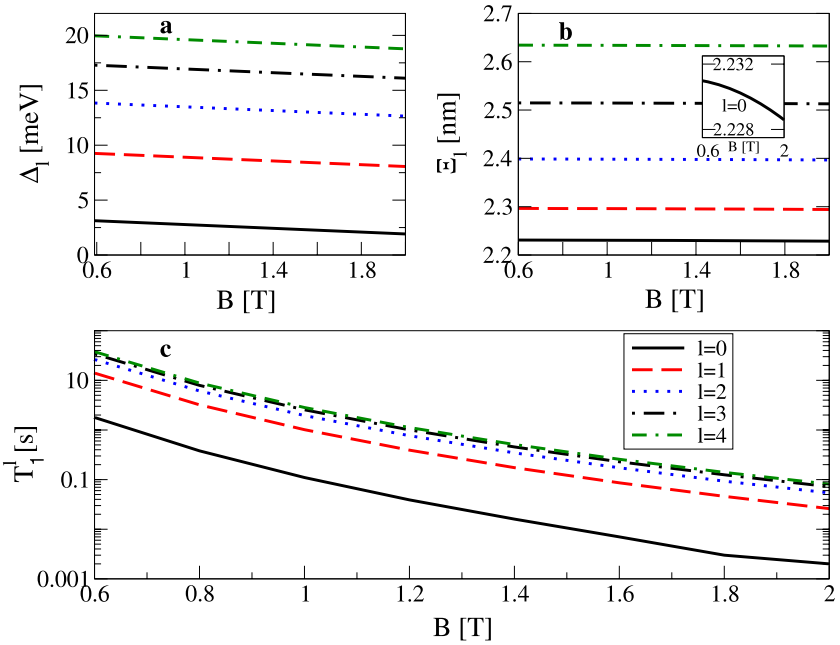

Figure 3. (a) The orbital energy gap Δ_l as a function of the magnetic field $B = B_\perp$, for different values of l; (b) the overlap factor Ξ_l; the inset plot shows the detailed curve $l = 0$ and (c) the relaxation time T_1^l. The remaining parameters are $k = 0.95$ and $r_0 = 14$ nm.

Table 2. The relaxation time T_1^l for different values of the orbital number l (equivalently, the number of electrons N_e) and different shapes of the potential $V_2(r)$. $r_0 = 14$ nm and $B_\parallel = 1$ T have been assumed.

	l				
k	0	1	2	3	4
0	8.03	2.01	0.89	0.50	0.32
0.5	1.55	0.83	0.52	0.35	0.26
0.7	0.67	0.78	0.64	0.51	0.41
0.9	0.27	1.11	1.54	1.64	1.59
0.95	**0.20**	**1.26**	**2.28**	**2.91**	**3.19**
1D QR	0.13	1.18	3.25	6.28	10.22

Table 3. The relaxation time T_1^l for different values of the orbital number l and the magnetic field $B_\perp$. $r_0 = 14$ nm and $k = 0.95$ have been assumed.

	l				
B (T)	0	1	2	3	4
0.6	1.789	14.035	26.390	34.093	37.754
0.8	0.38	3.209	6.110	7.933	8.809
1.0	**0.110**	**1.013**	**1.953**	**2.549**	**2.838**
1.6	0.007	0.086	0.173	0.229	0.257
2.0	0.002	0.026	0.054	0.072	0.081

(see figure 3 and table 3). To compare the results for $B_\parallel = 1$ T and $B_\perp = 1$ T see the seventh row in table 2 and the third row in table 3 (bold rows).

We would like to stress that spins from higher Bohm–Aharonov minima have much shorter relaxation times due to increasing $B_\perp$ and are uninteresting for our purposes. It results from the strong decrease of T_1 with increasing magnetic field (equation (14)).

The above model considerations have been done for InGaAs/GaAs rings but the underlying physics is similar to other systems with somehow different sets of parameters. In GaAs and GaAs/AlGaAs nanosystems the spin g_s factor changes in a range $g_s \sim 0.2$–0.4 [5]. Assuming that material properties entering equation (14) are roughly the same as for InGaAs/GaAs and $N_e = 1$ we obtain, for example, for ring B made out of material with $g_s = 0.4$, $T_1 \sim 6.4$ s and for ring C with $g_s = 0.4$, $T_1 \sim 43$ s.

These very long relaxation times have been obtained taking into account only SO-mediated interactions with piezoelectric phonons. However, other mechanisms of relaxation, (e.g. due to fluctuations of the electric and magnetic fields, deformational phonons, multiphonon processes and circuit noise) which we neglected in the above model calculations, can further limit the relaxation time.

The spin decoherence time T_2 in group III–V nanosystems is limited by HFI, as it was shown in [17] that SOI does not lead to pure dephasing. Several strategies have been proposed to decrease the randomness in the nuclear-spin system and reducing electron spin dephasing which can be useful also for QRs. Dynamic nuclear polarization [20] and putting the nuclear spins in a particular quantum state [21] are very promising. The decoherence times are in the range $T_2 \sim 10$–100 μs for the considered magnetic field.

If QRs were made of group IV isotopes with zero nuclear spins, the coherence times should be longer because of the absence or very small (in isotopically not purified) hyperfine interactions. In this context carbon nanotube QRs are also attractive because of the zero nuclear spin of the dominant isotope ^{12}C [22, 23]. Because of the ubiquitous nature of Si in modern electronics the estimations for Si rings [24] are important. It is known that the magnitude of the SOI in Si is ten times smaller than in GaAs and thus the relaxation times

should be a hundred times longer. However, for Si and SiGe systems $g_s \sim 2$ and these two factors make T_1 of the same order as for GaInAs rings. All these systems should have long decoherence times $T_2 = 2T_1$ due to the absence of nuclear spins.

4. Spin qubit on a quantum ring

Long relaxation (and decoherence) times obtained in our model calculations show that stable spin states are present both in QDs and QRs. Thus prerequisites for treating them as qubits are met in both structures. During the past few years great progress has been made towards full control of quantum states of single and coupled spins in QDs [5, 15, 25]. Going carefully through all this one finds that most of those features are shared also by QRs. Below we briefly discuss how to perform single qubit operations and to implement efficient quantum logic gates on pairs of QR qubits.

The qubit built on an electrostatically defined QR (EQR) can be initialized by, for example, thermal equilibration. Driven coherent spin rotations (Rabi oscillations) can be performed through magnetic resonance technique or by faster electric fields [15]. The electron spin can be measured by spin to charge conversion with the electron charge detected using a nearby quantum point contact [5, 26]. Coherent coupling of EQRs leading to the formation of, for example, the CNOT gate can be obtained in an analogous way as for QDs [1, 2] by assembling a system of two coplanar QRs with the possibility of tuning their exchange coupling J by gating the barrier between them. Such coupling can be switched on and off by electrical impulses.

Self-assembled QRs (SQRs) can be primarily controlled optically. Optical selection rules allow the initialization and read out of the spin states [11, 25]. Here the conversion of spin states into the polarization of light is used. Very fast coherent manipulations (Rabi oscillations) of single spins can be performed by optical techniques, e.g. by the a.c. Stark effect [15]. Quantum gates for SQRs can be accomplished by electronic or photonic connections [11, 12, 25]. Recently a scheme for creating coherent coupling of spin qubits, each placed in a microcavity, by entanglement swapping [27] has been proposed. Single qubit rotations together with the CNOT gate form an universal set of quantum logic gates. Remarkably these operations are very fast, of the order of pico- to nanoseconds [28]. Thus very many coherent operations can be performed during the estimated decoherence times allowing for the quantum error correction scheme to be efficient.

5. Discussion

Quantum rings have long fascinated physicists. Just like QDs, QRs possess atom-like properties, making them attractive for quantum information processing.

We have calculated relaxation times for QRs which turned out to be different than in QDs due to the different confinement. We have shown that the detailed shape and distribution of the radial parts of the wavefunctions highly determine the relaxation times. In order to describe this dependence we introduced a quantity, namely the overlap factor Ξ, that directly enters the expression for the relaxation time and, at the same time, can be easily calculated numerically for an arbitrary confining potential. This way, it can give a suggestion concerning a possible application of a given system as a qubit. In our calculations we used the harmonic potential for both QRs and QDs. It is, however, possible to produce nanostructures in which electrons are confined by potentials of other shapes, e.g. with rectangular cross sections. Though we have not carried out calculations for such systems, one can easily calculate the overlap factor and evaluate whether they may be useful to build qubits.

Detailed analysis have shown that for singly occupied structures QDs always have longer relaxation times than QRs (assuming the same material parameters) but for relatively thin rings with higher occupation the relaxation times can exceed those for QDs (due to the increased size of the energy gaps).

The estimated relaxation times (at $B = 1$ T) for experimentally fabricated rings (see table 1) are in the range between a few milliseconds to a few seconds. We have also calculated the relaxation times for a set of QRs with different radii and thicknesses. It follows that even singly occupied rings with $r_0 \leqslant 12$ nm can have relaxation times exceeding seconds.

The successful realization of the MBE-grown InAs QR structures, with a radius of 11.5 nm, has been reported in [10]. Another possibility for a practical realization of the QR structures with radii in the range of 10 nm or less is the combination of axial and radial heterostructures in semiconductor nanowires. They can easily be grown on pre-patterned substrates, i.e. they can be oriented in plane in periodical structures, defined by the patterning process [29]. Probably the combination of confinement due to the electric potential defined by metallic gates in the small sections of core–shell nanowire structures, already successfully applied to define a QD-like potential [30] seems, at present, to be the best method for realization of QR-type confinement with $r_0 < 10$ nm.

Based on the high stability of spin states in QRs we have proposed to build spin qubits on QRs. We have discussed that spins in QRs can be (in close analogy to QDs) initialized, manipulated, read out and coupled to each other, forming the universal set of quantum gates.

Finally, it should be stressed that multiply connected ring geometry offers additional (orbital) degrees of freedom to be used for quantum manipulations. It is possible to build a qubit on the orbital degrees of freedom [31, 32] in some analogy to flux qubits on superconducting rings. Thus quantum carrier confinement in circular nanostructures can be the basis of many applications in quantum information processing devices.

Acknowledgments

MMM acknowledges grant no. NN 202 128 736 from the Ministry of Science and Higher Education (Poland). EZ thanks T Dietl and W Jantsch for valuable discussions.

References

[1] Loss D and DiVincenzo D P 1998 *Phys. Rev.* A **57** 120

[2] Vandersypen L M K, Hanson R, Willems van Beveren L H, Elzerman J M, Greidanus J S, De Franceschi S and Kouwenhoven L P 2004 *Quantum Computing and Quantum Bits in Mesoscopic Systems* ed A Leggett, B Ruggiero and P Silvestrini (New York: Kluwer)

[3] Amasha S, MacLean K, Radu I P, Zumbühl D M, Kastner M A, Hanson M P and Gossard A C 2008 *Phys. Rev. Lett.* **100** 046803

[4] Kroutvar M, Ducommun Y, Heiss D, Bichler M, Schuh D, Abstreiter G and Finley J J 2004 *Nature* **432** 81

[5] Hanson R, Kouwenhoven L P, Petta J R, Tarucha S and Vandersypen L M K 2007 *Rev. Mod. Phys.* **79** 1217

[6] Fuhrer A, Scher S L, Ihn T, Henzel T, Ensslin K, Wegscheider W and Bichler M 2001 *Nature* **413** 822

[7] Baranwal V, Biasiol G, Heun S, Locatelli A, Mentes T O and Niño Orti M 2009 *Phys. Rev.* B **80** 155328

[8] Lei W, Notthoff C, Lorke A, Reuter D and Wieck A D 2010 *Appl. Phys. Lett.* **96** 033111

[9] Lorke A, Luyken R J, Govorov A O and Kotthaus J P 2000 *Phys. Rev. Lett.* **84** 2223

[10] Kleemans N A J M, Bominaar-Silkens I M A, Fomin V M, Gladilin V N, Granados D, Taboada A G, García J M, Offermans P, Zeitler U, Christianen P C M, Maan J C, Devreese J T and Koenraad P M 2009 *Phys. Rev. Lett.* **99** 146808

[11] Mano T, Kuroda T, Mitsuishi K, Yamagiwa M, Guo X-J, Furuya K, Sakoda K and Koguchi N 2007 *J. Cryst. Growth* **301** 740
Kuroda T, Mano T, Ochiai T, Sanguinetti S, Sakoda K, Kido G and Koguchi N 2005 *Phys. Rev.* B **72** 205301

[12] Abbarchi M, Mastrandrea C A, Vinattieri A, Sanguinetti S, Mano T, Kuroda T, Koguchi N, Sakoda K and Gurioli M 2009 *Phys. Rev.* B **79** 085308

[13] Räsänen E, Castro A, Werschnik J, Rubio A and Gross E K U 2007 *Phys. Rev. Lett.* **98** 157404

[14] Sælen L, Waltersson E, Hansen J P and Lindroth E 2010 *Phys. Rev.* B **81** 033303

[15] Hanson R and Awschalom D D 2008 *Nature* **453** 1043

[16] Khaetskii A V and Nazarov Y V 2001 *Phys. Rev.* B **64** 125316

[17] Golovach V N, Khaetskii A V and Loss D 2004 *Phys. Rev. Lett.* **93** 016601

[18] Halonen V, Pietiläinen P and Chakraborty T 1996 *Europhys. Lett.* **33** 377

[19] Dreiser J, Atatüre M, Galland C, Müller T, Badolato A and Imamoglu A 2008 *Phys. Rev.* B **77** 075317

[20] Xu X, Yao W, Sun B, Steel D G, Bracker A S, Gammon D and Sham L J 2009 *Nature* **459** 1105

[21] Giedke G, Taylor J M, D'Alessandro D, Lukin M D and Imamoglu A 2006 *Phys. Rev.* A **74** 032316

[22] Kuemmeth F, Ilani S, Ralph D C and McEuen P L 2008 *Nature* **452** 448

[23] Trauzettel B, Bulayev D V, Loss D and Burkhard G 2007 *Nat. Phys.* **3** 192

[24] Lee C-H, Liu C W, Chang H-T and Lee S W 2010 *J. Appl. Phys.* **107** 056103

[25] Ladd T D, Jelezko F, Laflamme R, Nakamura Y, Monroe C and O'Brien J L 2010 *Nature* **464** 45

[26] Elzerman J M, Hanson R, Willems van Beveren L H, Witkamp B, Vandersypen L M K and Kouwenhoven L P 2004 *Nature* **430** 431

[27] Kurpas M and Zipper E 2008 *Phys. J.* D **50** 201

[28] Zak R A, Röthlisberger B, Chesi S and Loss D 2010 *Riv. Nuovo Cimento* **033** 345

[29] Märtensson T, Carlberg P, Borgstrom M, Montelius L, Seifert W and Samuelson L 2004 *Nano Lett.* **4** 699

[30] Shtrikman H, Popovitz-Biro R, Kretinin A, Houben L, Heiblum M, Bukala M, Galicka M, Buczko R and Kacman P 2009 *Nano Lett.* **9** 1506

[31] Zipper E, Kurpas M, Szelag M, Dajka J and Szopa M 2006 *Phys. Rev.* B **74** 125426
Zipper E and Kurpas M 2010 *J. Comput. Theor. Nanosci.* **7** 1642

[32] Szopa M and Zipper E 2010 *J. Phys.: Conf. Ser.* **213** 012006